The Buckling of Thin Cylindrical Shells under Axial Compression

Theodore von Kármán and Hsue-shen Tsien
(*California Institute of Technology*)

In two previous papers[1,2] the authors have discussed in detail the inadequacy of the classical theory of thin shells in explaining the buckling phenomenon of cylindrical and spherical shells. It was shown that not only the calculated buckling load is 3 to 5 times higher than that found by experiments, but the observed wave pattern of the buckled shell is also different from that predicted. Furthermore, it was pointed out that the different explanations for this discrepancy advanced by L. H. Donnell[3] and W. Flügge[4] are untenable when certain conclusions drawn from these explanations are compared with the experimental facts. By a theoretical investigation on spherical shells[1] the authors were led to the belief that in general the buckling phenomenon of curved shells can only be explained by means of a non-linear large deflection theory. This point of view was substantiated by model experiments on slender columns with non-linear elastic support[2]. The non-linear characteristics of such structures cause the load necessary to keep the shell in equilibrium to drop very rapidly with increase in wave amplitude once the structure started to buckle. Thus, first of all, a part of the elastic energy stored in the shell is released once the buckling has started; this explains the observed rapidity of the buckling process. Furthermore, as it was shown in one of the previous papers[2] the buckling load itself can be materially reduced by slight imperfections in the test specimen and vibrations during the testing process.

In this paper, the same ideas are applied to the case of a thin uniform cylindrical shell under axial compression. First it is shown by an approximate calculation that again the load sustained by the shell drops with increasing deflection. Then the results of this calculation are used for a more detailed discussion of the buckling process as observed in an actual testing machine.

Stresses in the Median Surface and the expression for the Total Energy of the System

Let x and y be measured in the axial and the circumferential direction in the median surface of the undeformed cylindrical shell and u, v and w be the components of displacement of a

Received February 1, 1941.
Journal of the Aeronautical Sciences, vol. 8, pp. 303 – 312, 1941.

point on the median surface of the shell in the x-direction, the y-direction and the radial direction (Fig. 1). Then at an arbitrary point in the median surface the unit strains in the x and y-directions, ε_x, ε_y and the unit shear γ_{xy} can be expressed in the following forms, including

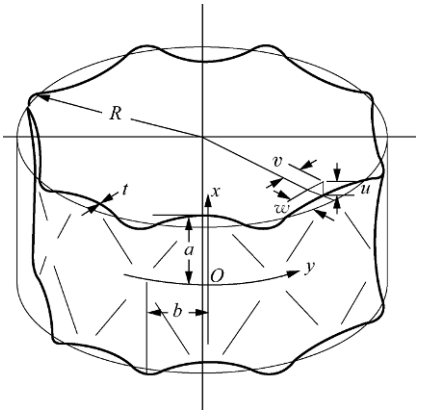


Fig. 1

terms up to second order:

$$\left.\begin{aligned}\varepsilon_x &= \frac{\partial u}{\partial x}+\frac{1}{2}\left(\frac{\partial w}{\partial x}\right)^2\\ \varepsilon_y &= \frac{\partial v}{\partial y}+\frac{1}{2}\left(\frac{\partial w}{\partial y}\right)^2-\frac{w}{R}\\ \gamma_{xy} &= \frac{\partial u}{\partial y}+\frac{\partial v}{\partial x}+\frac{\partial w}{\partial x}\frac{\partial w}{\partial y}\end{aligned}\right\} \tag{1}$$

R is the radius of the undeformed median surface of the shell. The stresses and the strains in the median surface of the shell are, however, related to each other by the following equations:

$$\left.\begin{aligned}\sigma_x &= \frac{E}{1-\nu^2}(\varepsilon_x+\nu\varepsilon_y)\\ \sigma_y &= \frac{E}{1-\nu^2}(\varepsilon_y+\nu\varepsilon_x)\\ \tau_{xy} &= \frac{E}{2(1+\nu)}\gamma_{xy}\end{aligned}\right\} \tag{2}$$

where E is Young's modulus of elasticity and ν is Poisson's ratio. Therefore, by substituting Eq. (1) into Eq. (2), the following connections between the components of stress in the median surface and the components of displacement of the median surface are obtained:

$$\left.\begin{aligned}\sigma_x &= \frac{E}{1-\nu^2}\left[\frac{\partial u}{\partial x}+\frac{1}{2}\left(\frac{\partial w}{\partial x}\right)^2+\nu\left\{\frac{\partial v}{\partial y}+\frac{1}{2}\left(\frac{\partial w}{\partial y}\right)^2-\frac{w}{R}\right\}\right]\\ \sigma_y &= \frac{E}{1-\nu^2}\left[\frac{\partial v}{\partial y}+\frac{1}{2}\left(\frac{\partial w}{\partial y}\right)^2-\frac{w}{R}+\nu\left\{\frac{\partial u}{\partial x}+\frac{1}{2}\left(\frac{\partial w}{\partial y}\right)^2\right\}\right]\\ \tau_{xy} &= \frac{E}{2(1+\nu)}\left[\frac{\partial u}{\partial y}+\frac{\partial v}{\partial x}+\frac{\partial w}{\partial x}\frac{\partial w}{\partial y}\right]\end{aligned}\right\} \tag{3}$$

It is generally accepted that the conditions of equilibrium between the stresses acting in the median surface of a thin shell can be approximately expressed by the equations used for flat plates:

$$\left.\begin{aligned}\frac{\partial \sigma_x}{\partial x}+\frac{\partial \tau_{xy}}{\partial y}=0\\ \frac{\partial \tau_{xy}}{\partial x}+\frac{\partial \sigma_y}{\partial y}=0\end{aligned}\right\} \tag{4}$$

This pair of equations can be satisfied by introducing the well known Airy's stress function, $F(x, y)$, defined by the relations

$$\sigma_x=\frac{\partial^2 F}{\partial y^2},\quad \tau_{xy}=-\frac{\partial^2 F}{\partial x\partial y},\quad \sigma_y=\frac{\partial^2 F}{\partial x^2} \tag{5}$$

Eliminating the variables u and v in Eqs. (3) and (5) the following relation between Airy's stress function $F(x, y)$ and the radial component of the displacement, w is obtained.

$$\left(\frac{\partial^2}{\partial x^2}+\frac{\partial^2}{\partial y^2}\right)^2 F=E\left[\left(\frac{\partial^2 w}{\partial x\partial y}\right)^2-\frac{\partial^2 w}{\partial x^2}\frac{\partial^2 w}{\partial y^2}-\frac{1}{R}\frac{\partial^2 w}{\partial x^2}\right] \tag{6}$$

This equation expresses the condition of compatibility between stress and strain. When $R\to\infty$, it reduces to the corresponding equation for a flat plate derived by the senior author[5]. L. H. Donnell[3] first obtained Eq. (6) in its present form. With a given distribution of the radial component of the displacement, w, Eq. (6) gives the induced stresses in the median surface of the shell.

For one complete wave panel, the extensional elastic energy W_1 corresponding to these stresses can be written as

$$W_1=\frac{t}{2E}4\int_0^a\int_0^b[(\sigma_x+\sigma_y)^2-2(1+\nu)(\sigma_x\sigma_y-\tau_{xy}^2)]\,\mathrm{d}x\mathrm{d}y\ ^* \tag{7}$$

where a and b are the half wave lengths in the axial and the circumferential directions, respectively.

To calculate the elastic energy of bending, it is necessary to find the expressions for the change of curvatures and the unit twist of the median surface. In this paper, the following simplified expressions will be used:

$$\chi_x=\frac{\partial^2 w}{\partial x^2},\quad \chi_{xy}=\frac{\partial^2 w}{\partial x\partial y},\quad \chi_y=\frac{\partial^2 w}{\partial y^2} \tag{8}$$

In Eq. (8), certain additional terms in χ_y and χ_{xy} involving v are neglected. It was shown by L. H. Donnell[6] that if the terms retained in Eq. (8) are considered as of the order one, the neglected terms are of the order $1/n^2$, where n is the number of waves in the circumferential direction. For thin cylindrical shells, the value of n is around 10; therefore the neglection is justified. With these expressions for the change of curvatures and the unit twist of the median surface, the bending energy W_2 for one complete wave panel can be written as

---

* The original: $W_1=\frac{t}{2E}4\int_0^a\int_0^b[(\sigma_x+\sigma_y)^2-2(1+\nu)(\sigma_x\sigma_y-\tau_{xy}^2)]\,\mathrm{d}\alpha\mathrm{d}y$.

$$W_2 = \frac{t^3 E}{24(1-\nu^2)} 4\int_0^a \int_0^b \left[\left\{ \frac{\partial^2 w}{\partial x^2} + \frac{\partial^2 w}{\partial y^2} \right\}^2 - 2(1-\nu)\left\{ \frac{\partial^2 w}{\partial x^2}\frac{\partial^2 w}{\partial y^2} - \left(\frac{\partial^2 w}{\partial x \partial y} \right)^2 \right\} \right] \mathrm{d}x\mathrm{d}y \tag{9}$$

The virtual work of the force applied on the end of the cylindrical shell can be calculated as the product of the applied force and the change in length of the shell. Therefore the following expression is obtained for one complete wave panel:

$$W_3 = 4t\int_0^b (\sigma_x)_{x=a} \mathrm{d}y \int_0^a \frac{\partial u}{\partial x} \mathrm{d}x \tag{10}$$

The equilibrium condition of the shell can be obtained either by equating the first variation of the difference between the sum of the energies W_1 and W_2 and the virtual work W_3 to zero, or by actually analyzing the moments and the stresses in the median surface of the shell. Using the approximations stated previously, Donnell[6] derived the equilibrium equation as

$$\frac{Et^3}{12(1-\nu^2)}\left(\frac{\partial^2}{\partial x^2} + \frac{\partial^2}{\partial y^2} \right)^4 w + \frac{Et}{R^2}\frac{\partial^4 w}{\partial x^4} = \left(\frac{\partial^2}{\partial x^2} + \frac{\partial^2}{\partial y^2} \right)^2 \left\{ p + t\left(\sigma_x \frac{\partial^2 w}{\partial x^2} + 2\tau_{xy}\frac{\partial^2 w}{\partial x \partial y} + \sigma_y \frac{\partial^2 w}{\partial x^2} \right) \right\} \tag{11}$$

where p is the external radial pressure on the surface of the shell. In the case concerned, $p = 0$, then using Eq. (5), the second equation connecting Airy's stress function $F(x, y)$ and the radial component of displacement w is obtained as

$$\frac{Et^2}{12(1-\nu^2)}\left(\frac{\partial^2}{\partial x^2} + \frac{\partial^2}{\partial y^2} \right)^4 w + \frac{E}{R^2}\frac{\partial^4 w}{\partial x^4} = \left(\frac{\partial^2}{\partial x^2} + \frac{\partial^2}{\partial y^2} \right)^2 \left[\frac{\partial^2 F}{\partial y^2}\frac{\partial^2 w}{\partial x^2} - 2\frac{\partial^2 F}{\partial x \partial y}\frac{\partial^2 w}{\partial x \partial y} + \frac{\partial^2 F}{\partial x^2}\frac{\partial^2 w}{\partial y^2} \right] \tag{12}$$

When $R \to \infty$, Eq. (12) reduces to the corresponding equation for a flat plate.

There are two different ways to solve the problem of buckling of a thin uniform cylindrical shell under axial compression. The more exact method is to solve Eqs. (6) and (12) simultaneously, using appropriate boundary conditions. The approximate method is to first assume a plausible function for w, with undetermined parameters and then use Eq. (6) to determine the stresses in the median surface of the shell. The expressions W_1, W_2 and W_3 can then be calculated by means of Eqs. (7), (9) and (10). The undetermined parameters can be ascertained by the condition that $W_1 + W_2 - W_3$ must be a minimum. This approximate method will be used in the following calculations.

Calculation of the Total Energy

To obtain a plausible form for w, one has to resort to the experimental results. It is observed that, for large values of the wave amplitude, the waves show a so-called diamond shaped pattern. This particular wave shape can be approximately expressed by

$$\frac{w_1}{R} = \cos^2 \frac{(mx+ny)}{2R} \cos^2 \frac{(mx-ny)}{2R} \tag{13}$$

where the squares are introduced to account for the fact that the shell has a definite preference to buckle inward. Eq. (13) can be re-written as

$$\frac{w_1}{R} = \frac{1}{4} + \frac{1}{2}\left[\cos\frac{mx}{R}\cos\frac{ny}{R} + \frac{1}{4}\cos\frac{2mx}{R} + \frac{1}{4}\cos\frac{2ny}{R}\right] \tag{14}$$

On the other hand, the classical theory which is correct for infinitesimal values of the wave amplitude requires the wave to be of the form

$$\frac{w_2}{R} = \cos\frac{mx}{R}\cos\frac{ny}{R} \tag{15}$$

In order to satisfy this requirement, the wave form assumed in the following calculation is

$$\frac{w}{R} = \left(f_0 + \frac{f_1}{4}\right) + \frac{f_1}{2}\left(\cos\frac{mx}{R}\cos\frac{ny}{R} + \frac{1}{4}\cos\frac{2mx}{R} + \frac{1}{4}\cos\frac{2ny}{R}\right) + \frac{f_2}{4}\left(\cos\frac{2mx}{R} + \cos\frac{2ny}{R}\right) \tag{16}$$

where f_0, f_1, f_2 are unknowns to be determined by the minimum condition given above; f_0 is introduced in order to allow the shell to expand radially. The amplitude of the wave pattern defined as the maximum difference in the radial deflection w is evidently given by f_1. The wave lengths in the axial and the circumferential direction are $2\pi R/m$ and $2\pi R/n$, respectively. Hence the number of waves along the circumference of the shell is equal to n. It is evident that no end effect can be accounted for by this form of wave pattern, and therefore the following calculation really corresponds to the case of a very long cylindrical shell. This simplification is justified by the experimental findings of N. Nojima and S. Kanemitsu as reported in a previous paper[2]. It was found that there is no appreciable length effect when the length of the cylindrical is greater than 1.5 times the radius of the shell. Furthermore, it is seen that by setting $f_0 = f_2 = 0$, Eq. (16) is reduced to Eq. (14); while by setting $(f_1/4)+(f_2/2) = 0$ and $f_0 + f_1/4 = 0$, Eq. (16) is reduced to Eq. (15). With other values of these parameters, wave patterns intermediate between these two limits can be obtained.

Substituting Eq. (16) into Eq. (6), the differential equation for Airy's stress function $F(x, y)$ is obtained:

$$\left(\frac{\partial^2}{\partial x^2} + \frac{\partial^2}{\partial y^2}\right)^2 F = -E\mu^2\left(\frac{n}{R}\right)^2\left[A\cos\frac{2mx}{R} + B\cos\frac{2ny}{R} + C\cos\frac{mx}{R}\cos\frac{ny}{R} + D\cos\frac{3mx}{R}\cos\frac{ny}{R} + G\cos\frac{mx}{R}\cos\frac{3ny}{R} + H\cos\frac{2mx}{R}\cos\frac{2ny}{R}\right] \tag{17}$$

where $\mu = m/n$, the "aspect ratio" of the waves. If $\mu > 1$, the waves are longer in the

circumferential direction; if $\mu<1$, the waves are longer in the axial direction. The coefficients in Eq. (17) are given by the following relations:

$$\left.\begin{aligned} A &= \frac{1}{8}f_1^2n^2-\left(\frac{1}{2}f_1+f_2\right)\\ B &= \frac{1}{8}f_1^2n^2\\ C &= \frac{1}{2}f_1n^2\left(\frac{1}{2}f_1+f_2\right)-\frac{1}{2}f_1\\ D &= \frac{1}{4}f_1n^2\left(\frac{1}{2}f_1+f_2\right)\\ G &= \frac{1}{4}f_1n^2\left(\frac{1}{2}f_1+f_2\right)\\ \text{and}\qquad H &= n^2\left(\frac{1}{2}f_1+f_2\right)^2 \end{aligned}\right\} \tag{18}$$

The solution of Eq. (17) can be easily obtained as

$$\begin{aligned} F=-E\mu^2\left(\frac{R}{n}\right)^2\Bigg[&\frac{A}{16\mu^4}\cos\frac{2mx}{R}+\frac{B}{16}\cos\frac{2ny}{R}+\frac{C}{(1+\mu^2)^2}\cos\frac{mx}{R}\cos\frac{ny}{R}+\\ &\frac{D}{(1+9\mu^2)^2}\cos\frac{3mx}{R}\cos\frac{ny}{R}+\frac{G}{(9+\mu^2)^2}\times\cos\frac{mx}{R}\cos\frac{3ny}{R}+\\ &\frac{H}{16(1+\mu^2)^2}\cos\frac{2mx}{R}\times\cos\frac{2ny}{R}\Bigg]+\frac{\alpha x^2}{2}+\frac{\beta y^2}{2} \end{aligned} \tag{19}$$

Using Eq. (5), the stress components in the median surface can be written as

$$\left.\begin{aligned} \sigma_x &= \overline{E}\mu^2\Bigg[\frac{B}{4}\cos\frac{2ny}{R}+\frac{C}{(1+\mu^2)^2}\cos\frac{mx}{R}\cos\frac{ny}{R}+\frac{D}{(1+9\mu^2)^2}\cos\frac{3mx}{R}\cos\frac{ny}{R}+\\ &\quad\frac{9G}{(9+\mu^2)^2}\cos\frac{mx}{R}\times\cos\frac{3ny}{R}+\frac{H}{4(1+\mu^2)^2}\cos\frac{2mx}{R}\cos\frac{2ny}{R}\Bigg]+\beta\\ \sigma_y &= E\mu^2\Bigg[\frac{A}{4\mu^2}\cos\frac{2mx}{R}+\frac{\mu^2C}{(1+\mu^2)^2}\cos\frac{mx}{R}\cos\frac{ny}{R}+\frac{9\mu^2}{(1+9\mu^2)^2}\cos\frac{3mx}{R}\cos\frac{ny}{R}+\\ &\quad\frac{\mu^2G}{(9+\mu^2)^2}\cos\frac{mx}{R}\times\cos\frac{3ny}{R}+\frac{\mu^2H}{4(1+\mu^2)^2}\cos\frac{2mx}{R}\cos\frac{2ny}{R}\Bigg]+\alpha\\ t_{xy} &= E\mu^2\Bigg[\frac{\mu C}{(1+\mu^2)^2}\sin\frac{mx}{R}\sin\frac{ny}{R}+\frac{3\mu D}{(1+9\mu^2)^2}\sin\frac{3mx}{R}\sin\frac{ny}{R}+\\ &\quad\frac{3\mu G}{(9+\mu^2)^2}\sin\frac{mx}{R}\sin\frac{3ny}{R}+\frac{\mu H}{4(1+\mu^2)^2}\sin\frac{2mx}{R}\sin\frac{2ny}{R}\Bigg] \end{aligned}\right\} \tag{20}$$

In all experimental work, the data are usually expressed in terms of the average compression stress σ in the axial direction. It can be easily seen from Eq. (20) that

$$\beta=-\sigma \tag{21}$$

Using Eq. (3), the following expressions for $\partial u/\partial x$ and $\partial v/\partial y$ can be obtained:

$$\begin{aligned}\frac{\partial u}{\partial x} &= \frac{1}{E}(\sigma_x - \nu\sigma_y) - \frac{1}{2}\left(\frac{\partial w}{\partial x}\right)^2 \\ \frac{\partial v}{\partial y} &= \frac{1}{E}(\sigma_y - \nu\sigma_x) - \frac{1}{2}\left(\frac{\partial w}{\partial y}\right)^2 + \frac{w}{R}\end{aligned} \tag{22}$$

By substituting Eqs. (16) and (20) into Eq. (22), it is found that

$$\begin{aligned}\frac{\partial u}{\partial x} &= -\left[\left(\frac{\sigma}{E} + \nu\frac{\alpha}{E}\right) + \frac{1}{2}n^2\mu^2\left(\frac{3}{32}f_1^2 + \frac{1}{8}f_1f_2 + \frac{1}{8}f_2^2\right)\right] + \\ &\quad \text{Terms of periodic functions} \\ \frac{\partial v}{\partial y} &= \frac{\alpha}{E} + \nu\frac{\sigma}{E} - \frac{1}{2}n^2\left(\frac{3}{32}f_1^2 + \frac{1}{8}f_1f_2 + \frac{1}{8}f_2^2\right) + \left(f_0 + \frac{f_1}{4}\right) + \\ &\quad \text{Terms of periodic functions}\end{aligned} \tag{23}$$

Since y is measured along the circumference of the shell, v must be a periodic function of y; therefore, the constant term in $\dfrac{\partial v}{\partial y}$ must be equal to zero. Or

$$\frac{\alpha}{E} + \nu\frac{\sigma}{E} - \frac{1}{2}n^2\left(\frac{3}{32}f_1^2 + \frac{1}{8}f_1f_2 + \frac{1}{8}f_2^2\right) + \left(f_0 + \frac{f_1}{4}\right) = 0 \tag{24}$$

This condition determines α.

Using Eqs. (7), (20) and (24), the extensional energy W_1 of the shell is obtained as

$$\begin{aligned}\frac{W_1}{\frac{1}{2}Etab} &= 4\Big[(1-\nu^2)\left(\frac{\sigma}{E}\right)^2 + n^4\left(\frac{3}{64}f_1^2 + \frac{1}{16}f_1f_2 + \right. \\ &\quad \left.\frac{1}{16}f_2^2\right)^2 + \left(f_0 + \frac{1}{4}f_1\right)^2 - 2n^2\left(\frac{3}{64}f_1^2 + \frac{1}{16}f_1f_2 + \right. \\ &\quad \left.\frac{1}{16}f_2^2\right)\left(f_0 + \frac{1}{4}f_1\right)\Big] + \Big[\frac{A^2}{8} + \frac{B^2\mu^4}{8} + \frac{\mu^4C^2}{(1+\mu^2)^2} + \\ &\quad \frac{\mu^4D^2}{(1+9\mu^2)^2} + \frac{\mu^4G^2}{(9+\mu^2)^2} + \frac{\mu^4H^2}{16(1+\mu^2)^2}\Big]\end{aligned} \tag{25}$$

Using Eqs. (9) and (16), the energy of bending W_2 of the shell can be calculated as

$$\begin{aligned}\frac{W_2}{\frac{1}{2}Etab} &= \frac{1}{6(1-\nu^2)}\left(\frac{t}{R}\right)^2 n^4\Big[f_1^2\left\{\frac{1}{8}(1+\mu^2)^2 + \frac{1}{4}(1+\mu^4)\right\} + \\ &\quad (1+\mu^4)f_1f_2 + (1+\mu^4)f_2^2\Big]\end{aligned} \tag{26}$$

The virtual work of the applied force can be obtained by means of Eqs. (10), (20), (23) and (24). The result is

$$\begin{aligned}\frac{W_3}{\frac{1}{2}Etab} &= \Big[2(1-\nu^2)\left(\frac{\sigma}{E}\right)^2 + n^2\,\frac{\sigma}{E}(\nu+\mu^2)\left\{\frac{3}{32}f_1^2 + \frac{1}{8}f_1f_2 + \frac{1}{8}f_2^2\right\} - \\ &\quad 2\nu\,\frac{\sigma}{E}\left(f_0 + \frac{1}{4}f_1\right)\Big]\end{aligned} \tag{27}$$

Relation Between the compression Stress and the Amplitude of Waves

To find the relation between the average compression stress and the amplitude of the waves, the conditions which will make the expression $W_1 + W_2 - W_3$ a minimum have to be obtained. It was found that the calculations can be simplified to a certain extent by first using the condition that the sum of energies must be minimum with respect to f_0. Or

$$\frac{\partial}{\partial f_0}(W_1 + W_2 - W_3) = 0 \tag{28}$$

This condition determines a relation between f_0 and f_1, f_2, which can be written as:

$$f_0 + \frac{1}{4}f_1 = n^2\left(\frac{3}{64}f_1^2 + \frac{1}{16}f_1 f_2 + \frac{1}{16}f_2^2\right) - \nu\frac{\sigma}{E} \tag{29}$$

Using this relation and Eq. (24), it is easily seen that $\alpha = 0$. In other words, the shell will expand radially to such an extent that the average of the circumferential stress σ_y is equal to zero. Substituting Eq. (29) into the expressions for W_1, W_2 and W_3 as given by Eqs. (25), (26) and (27) and using Eq. (18), the elastic energy of the system minus the virtual work is expressed finally in the following form:

$$\begin{aligned}\frac{W_1 + W_2 - W_3}{\frac{1}{2}Etab} = &-4\left(\frac{\sigma}{E}\right)^2 - \frac{\sigma}{E}n^2\mu^2\left(\frac{3}{8}f_1^2 + \frac{1}{2}f_1 f_2 + \frac{1}{2}f_2^2\right) + \\ &n^4\left[\left\{\frac{1+\mu^4}{512} + \frac{17}{256}\frac{\mu^4}{(1+\mu^2)^2} + \frac{1}{64}\frac{\mu^4}{(1+9\mu^2)^2} + \frac{1}{64}\frac{\mu^4}{(9+\mu^2)^2}\right\}f_1^4 + \right. \\ &\left\{\frac{9}{32}\frac{\mu^4}{(1+\mu^2)^2} + \frac{1}{16}\frac{\mu^4}{(1+9\mu^2)^2} + \frac{1}{16}\frac{\mu^4}{(9+\mu^2)^2}\right\}f_1^3 f_2 + \\ &\left\{\frac{11}{32}\frac{\mu^4}{(1+\mu^2)^2} + \frac{1}{16}\frac{\mu^4}{(1+9\mu^2)^2} + \frac{1}{16}\frac{\mu^4}{(9+\mu^2)^2}\right\}f_1^2 f_2^2 + \\ &\left.\frac{1}{8}\frac{\mu^4}{(1+\mu^2)^2}f_1 f_2^3 + \frac{1}{16}\frac{\mu^4}{(1+\mu^2)^2}f_2^4\right] - n^2\left[\left\{\frac{1}{64} + \frac{1}{4}\frac{\mu^4}{(1+\mu^2)^2}\right\}f_1^3 + \right. \\ &\left.\left\{\frac{1}{32} + \frac{1}{2}\frac{\mu^4}{(1+\mu^2)^2}\right\}f_1^2 f_2\right] + \left[\left\{\frac{1}{32} + \frac{1}{4}\frac{\mu^4}{(1+\mu^2)^2}\right\}f_1^2 + \frac{1}{8}f_1 f_2 + \right. \\ &\left.\frac{1}{8}f_2^2\right] + \frac{1}{6(1-\nu^2)}\left(\frac{t}{R}\right)^2 n^4\left[\left\{\frac{1}{8}(1+\mu^2)^2 + \frac{1}{4}(1+\mu^4)\right\}f_1^2 + \right. \\ &\left.(1+\mu^4)f_1 f_2 + (1+\mu^4)f_2^2\right]\end{aligned} \tag{30}$$

The equilibrium conditions are then obtained by differentiating this expression with respect to f_1 and f_2, and then set those derivatives equal to zero. The results can be written in a simpler form by introducing the following parameters:

$$\rho = \frac{f_2}{f_1}, \quad \eta = n^2\frac{t}{R}, \quad \xi = f_1\frac{R}{t} = \frac{\delta}{t} \tag{31}$$

where δ is the wave amplitude of the buckled shape of the cylindrical shell. Then the

equilibrium conditions are

$$\left.\begin{aligned}
\left(\frac{\sigma R}{Et}\eta\mu^2\left(\rho+\frac{3}{2}\right)\right.&=(\eta\xi)^2\left[\frac{\mu^4}{4(1+\mu^2)^2}\rho^3+\right.\\
&\left\{\frac{11}{8}\frac{\mu^4}{(1+\mu^2)^2}+\frac{1}{4}\frac{\mu^4}{(1+9\mu^2)^2}+\frac{1}{4}\frac{\mu^4}{(9+\mu^2)^2}\right\}\rho^2+\\
&\left\{\frac{27}{16}\frac{\mu^4}{(1+\mu^2)^2}+\frac{3}{8}\frac{\mu^4}{(1+9\mu^2)^2}+\frac{3}{8}\frac{\mu^4}{(9+\mu^2)^2}\right\}\rho+\\
&\left.\left\{\frac{1+\mu^4}{64}+\frac{17}{32}\frac{\mu^4}{(1+\mu^2)^2}+\frac{1}{8}\frac{\mu^4}{(1+9\mu^2)^2}+\frac{1}{8}\frac{\mu^4}{(9+\mu^2)^2}\right\}\right]-\\
&(\eta\xi)\left[\left\{\frac{1}{8}+2\frac{\mu^4}{(1+\mu^2)^2}\right\}\rho+\left\{\frac{3}{32}+\frac{3}{2}\frac{\mu^4}{(1+\mu^2)^2}\right\}\right]+\\
&\left[\frac{1}{4}\rho+\left\{\frac{1}{8}+\frac{\mu^4}{(1+\mu^2)^2}\right\}\right]+\frac{1}{3(1-\nu^2)}\eta^2\left[(1+\mu^4)\rho+\right.\\
&\left.\left\{\frac{1}{4}(1+\mu^2)^2+\frac{1}{2}(1+\mu^4)\right\}\right]\\
\frac{\sigma R}{Et}\eta\mu^2\left(\rho+\frac{1}{2}\right)&=(\eta\xi)^2\left[\frac{1}{4}\frac{\mu^4}{(1+\mu^2)^2}\rho^3+\frac{3}{8}\frac{\mu^4}{(1+\mu^2)^2}\rho^2+\right.\\
&\left\{\frac{11}{16}\frac{\mu^4}{(1+\mu^2)^2}+\frac{1}{8}\frac{\mu^4}{(1+9\mu^2)^2}+\frac{1}{8}\frac{\mu^4}{(9+\mu^2)^2}\right\}\rho+\\
&\left.\left\{\frac{9}{32}\frac{\mu^4}{(1+\mu^2)^2}+\frac{1}{16}\frac{\mu^4}{(1+9\mu^2)^2}+\frac{1}{16}\frac{\mu^4}{(9+\mu^2)^2}\right\}\right]-\\
&(\eta\xi)\left[\frac{1}{32}+\frac{1}{2}\frac{\mu^4}{(1+\mu^2)^2}\right]+\left[\frac{1}{4}\rho+\frac{1}{8}\right]+\\
&\frac{1}{3(1-\nu^2)}\eta^2\left[(1+\mu^4)\rho+\frac{1}{2}(1+\mu^4)\right]
\end{aligned}\right\}\tag{32}$$

Eliminating $\sigma R/(Et)$ from the above equations, the following equation for ρ is obtained

$$A_3\rho^3+A_2\rho^2+A_1\rho+A_0=0\tag{33}$$

where the coefficients are

$$\left.\begin{aligned}
A_3&=(\eta\xi)^2\left\{\frac{3\mu^4}{(1+\mu^2)^2}+\frac{\mu^4}{(1+9\mu^2)^2}+\frac{\mu^4}{(9+\mu^2)^2}\right\}\\
A_2&=(\eta\xi)^2\left\{\frac{9}{2}\frac{\mu^4}{(1+\mu^2)^2}+\frac{3}{2}\frac{\mu^4}{(1+9\mu^2)^2}+\frac{3}{2}\frac{\mu^4}{(9+\mu^2)^2}\right\}-(\eta\xi)\left\{\frac{1}{2}+\frac{8\mu^4}{(1+\mu^2)^2}\right\}\\
A_1&=(\eta\xi)^2\left\{\frac{1+\mu^4}{16}+\frac{1}{4}\frac{\mu^4}{(1+\mu^2)^2}+\frac{1}{4}\frac{\mu^4}{(1+9\mu^2)^2}+\frac{1}{4}\frac{\mu^4}{(9+\mu^2)^2}\right\}-\\
&\quad(\eta\xi)\left\{\frac{1}{2}+\frac{8\mu^4}{(1+\mu^2)^2}\right\}+\left\{\frac{4\mu^4}{(1+\mu^2)^2}-1\right\}-\frac{2}{3(1-\nu^2)}\eta^2\times\\
&\quad\left\{2(1+\mu^4)-\frac{1}{2}(1+\mu^2)^2\right\}\\
A_0&=(\eta\xi)^2\left\{\frac{1+\mu^4}{32}-\frac{5}{8}\frac{\mu^4}{(1+\mu^2)^2}-\frac{1}{8}\frac{\mu^4}{(1+9\mu^2)^2}-\frac{1}{8}\frac{\mu^4}{(9+\mu^2)^2}\right\}+\\
&\quad\left\{\frac{2\mu^4}{(1+\mu^2)^2}-\frac{1}{2}\right\}-\frac{2}{3(1-\nu^2)}\eta^2\left\{(1+\mu^4)-\frac{1}{4}(1+\mu^2)^2\right\}
\end{aligned}\right\}\tag{34}$$

Therefore, when $\xi = 0$, i.e., when the wave amplitude approaches zero Eq. (32) gives $A_2 = A_3 = 0$; and

$$A_1 = -\frac{2}{3(1-\nu^2)}\eta^2\left\{2(1+\mu^4) - \frac{1}{2}(1+\mu^2)^2\right\}$$

$$A_0 = -\frac{2}{3(1-\nu^2)}\eta^2\left\{(1+\mu^4) - \frac{1}{4}(1+\mu^2)^2\right\}$$

$$= \frac{A_1}{2}$$

Substituting into Eq. (31) it is seen that $\rho = -1/2$, or $f_2 = -1/2f_1$. Putting this relation between f_1 and f_2 into Eq. (14), the wave pattern is reduced to that represented by Eq. (15)*, i.e., the wave pattern for infinitesimal wave amplitude given by the classical theory.

With a given value of μ and η, the coefficients for various values of the wave amplitude ξ can be first calculated by using Eq. (34). Then Eq. (33) can be solved for ρ corresponding to this particular set of values of μ and η at various wave amplitude ξ. When the value of ρ is known, Eq. (32) can be used to calculate the corresponding value of the "reduced compression stress," $\sigma R/(Et)$. It is found, however, that the following expression which is obtained from Eq. (30) by eliminating the third powers of ρ is more suitable for numerical computations:

$$\frac{\sigma R}{Et} = \left\{\frac{1}{\eta}\frac{\mu^2}{(1+\mu^2)^2} + \frac{1}{12(1-\nu^2)}\frac{\eta(1+\mu^2)^2}{\mu^2}\right\} +$$
$$\frac{1}{\eta\mu^2}\Bigg[(\eta\xi)^2\left\{\frac{\mu^4}{(1+\mu^2)^2} + \frac{\mu^4}{4(1+9\mu^2)^2} + \frac{\mu^4}{4(9+\mu^2)^2}\right\}\rho^2 +$$
$$\left\{(\eta\xi)^2\left(\frac{\mu^4}{(1+\mu^2)^2} + \frac{1}{4}\frac{\mu^4}{(1+9\mu^2)^2} + \frac{1}{4}\frac{\mu^4}{(9+\mu^2)^2}\right) -\right.$$
$$\left.(\eta\xi)\left(\frac{1}{8} + \frac{2\mu^4}{(1+\mu^2)^2}\right)\right\}\rho + \left\{(\eta\xi)^2\left(\frac{1+\mu^4}{64} + \frac{1}{4}\frac{\mu^4}{(1+\mu^2)^2} +\right.\right.$$
$$\left.\left.\frac{1}{16}\frac{\mu^4}{(1+9\mu^2)^2} + \frac{1}{16}\frac{\mu^4}{(9+\mu^2)^2}\right) - (\eta\xi)\left(\frac{1}{16} + \frac{\mu^4}{(1+\mu^2)^2}\right)\right\}\Bigg] \tag{35}$$

Therefore, when $\xi \to 0$, i.e., when the wave amplitude becomes very small, Eq. (35) reduces to

$$\left(\frac{\sigma R}{Et}\right)_{\xi\to 0} = \frac{1}{\eta}\frac{\mu^2}{(1+\mu^2)^2} +$$
$$\frac{1}{12(1-\nu^2)}\frac{1}{\dfrac{1}{\eta}\dfrac{\mu^2}{(1+\mu^2)^2}} \tag{36}$$

The minimum value of the average compression stress σ is given by

$$\text{Min.}\left(\frac{\sigma R}{Et}\right)_{\xi\to 0} = \frac{1}{\sqrt{3(1-\nu^2)}} \tag{37}$$

---

* Eq. (15) in original paper has been corrected as Eq. (13). — Noted by editor

which is the well known result from the classical theory of infinitesimal deflections. This minimum value is obtained when

$$\eta \frac{(1+\mu^2)^2}{\mu^2} = 2\sqrt{3(1-\nu^2)} \tag{38}$$

It is interesting to notice that for infinitesimal wave amplitude, the minimum value of average compression stress occurs for an infinite number of pairs of the values of the parameters η and μ, for which the combined parameter shown in Eq. (38) has the same value.

Numerical computations were carried out for two values of the parameter μ, the ratio of the wave lengths in circumferential direction and in axial direction. These values of μ are 1 and 0.5. The value 1 was chosen because the experiments indicate that at large values of wave amplitude, the diamond waves have almost equal sides. The value 0.5 was chosen to investigate the possibility of occurrence of narrow waves. The results of these computations are shown in Fig. 2 and Fig. 3, where the reduced compression stress $\sigma R/(Et)$ is plotted against the wave amplitudes ξ. The parameter in the figures is η. The values written in the parenthesis after η are the actual number of waves n in circumferential direction for $R/t = 1000$. For given values of η and μ, i.e., a fixed side of the wave, the load sustained by the shell, $\sigma R/(Et)$ first decreases as the wave amplitude, ξ, is increased. After a minimum is reached, the load will rise with increase in wave amplitude. When the waves are larger, the initial buckling load, i.e., the value of $\sigma R/(Et)$ at $\xi = 0$, is higher. However, the minimum load reached tends to a lower value, except for $\eta < 0.169$ and $\mu = 1$. For $\mu = 0.5$, the lowest value of the minimum load is not yet reached at $\eta = 0.081$.

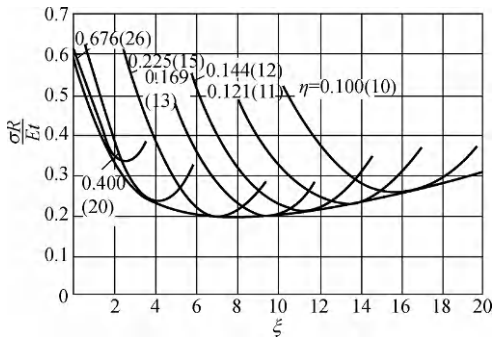


Fig. 2 Reduced compression stress $\sigma R/(Et)$ against amplitude of waves $\xi = \delta/t$, for $\mu = 1.00$ and different number of waves in circumferential direction

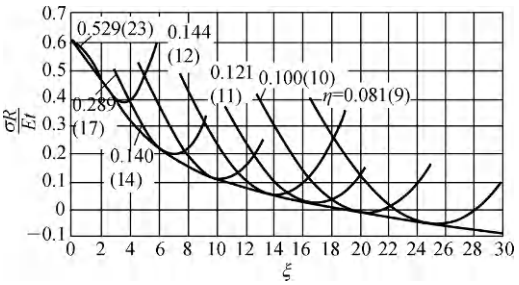


Fig. 3 Reduced compression stress $\sigma R/(Et)$ against amplitude of waves $\xi = \delta/t$, for $\mu = 0.50$ and different number of waves in circumferential direction

The Relation Between the Compression Stress and the Shortening of the Shell in the Axial Direction

Although the load characteristic of the cylindrical shell shown in the Figs. 2 and 3 gives the

possible equilibrium relations between load and amplitude of the deflection wave, the actual behavior of a specimen in a testing machine cannot be directly seen from these figures. In a testing machine, the only factor under the control of the operator is the distance between the end plates; this is the geometrical restraint with which the specimen must conform. Therefore, in order to determine the behavior of the specimen the compression stress will have to be plotted as function of the end shortening. The unit end shortening, ε, i. e., the total shortening in one wave length of the shell in axial direction divided by the wave length, can be easily calculated from Eq. (23). It is found that

$$\frac{\varepsilon R}{t} = \frac{\sigma R}{Et} + \frac{\mu^2}{16}\xi(\eta\xi)\left(\rho^2 + \rho + \frac{3}{4}\right) \tag{39}$$

This equation for the unit end shortening contains only quantities already found such as the values of ρ and $\sigma R/(Et)$. In Figs. 4 and 5, $\sigma R/(Et)$ is plotted against $\varepsilon R/t$ for $\mu = 1$ and $\mu = 0.5$, respectively. It is immediately clear from these two figures that if the buckling process follows the curves drawn, after the shell starts to buckle the end shortening has to decrease. In other words, the end plates of the testing machine have to move apart. Therefore, the process of buckling in this region is highly unstable; as a matter of fact, before the operator has time to separate the end plates, the shell will jump to the point P (Fig. 4 or 5) which corresponds to the same end shortening as the starting point of the buckling process, but to a much lower compression stress. This jump in equilibrium position involves a release of elastic energy and thus explains the rapidity of the buckling process and the accompaning vibration.

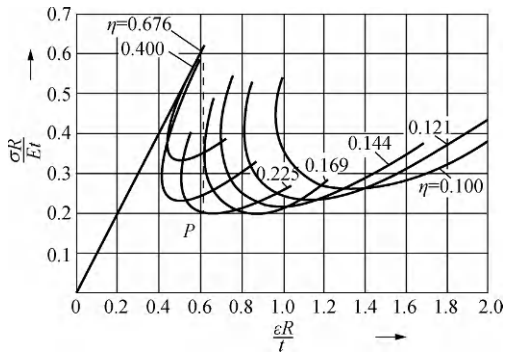


Fig. 4 Reduced compression stress $\sigma R/(Et)$ against unit end shortening $\varepsilon R/t$, for $\mu = 1.00$ and different number of waves in circumferential direction

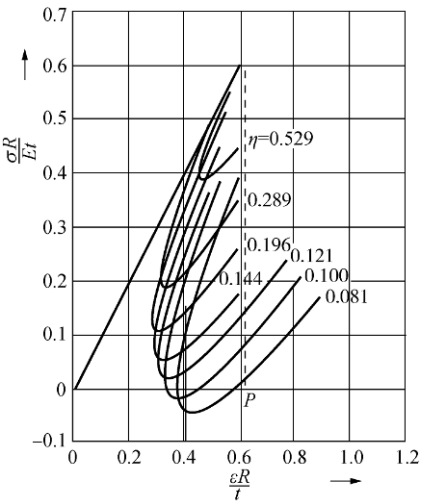


Fig. 5 Reduced compression stress $\sigma R/(Et)$ against unit end shortening $\varepsilon R/t$, for $\mu = 0.50$ and different number of waves in circumferential direction

It is tacitly assumed in the previous paragraph that if the system has an equilibrium

position corresponding to the same end conditions, i.e., same end shortening, but involving a lower value of σ or a lower value of the stored elastic energy, a transition to one of these equilibrium positions will actually take place. This is not based on any vigorous application of the principles of mechanics. It is evident that if, for example, the straight equilibrium position is stable, i.e., all infinitesimally near configurations have higher energy, such a transition can only take place by application of an external impulse of finite magnitude. However, it can be assumed that such impulses will always be present in an experiment performed without extraordinary precaution in this respect, and of course if the structure is used in service. Then again, if it is assumed that the structure is helped over the "energy hump" by such external impulse, it cannot be proved that the jump has to end in the equilibrium position with the lowest energy level. However, if it is exposed to several random impulses, there is a certain probability that the position with the lowest energy level will be the "journey's end." An approximate calculation of the elastic energy of the shells shows that for large values of $\varepsilon R/t$ and $\eta < 0.121$, the elastic energy of the narrow waves is higher than that of the square waves at same value of the end shortening. Therefore, under such conditions the narrow waves appear to be less probable. However, for $\varepsilon R/t$ near 0.6, and $\eta \geqslant 0.121$ the elastic energy stored in the shell for the narrow waves is comparable to that for the square waves at the same value of the end shortening. This indicates the possibility of the appearance of narrow waves during the very initial stages of the buckling process.

In any case, it is certain that there are equilibrium positions of a buckled cylindrical shell which involve much lower average compression stress $\sigma R/(Et)$ than that at the beginning of buckling. For instance, in the case of square wave pattern, the lowest compression stress is given by

$$\frac{\sigma}{E} = 0.194\,\frac{t}{R} \tag{40}$$

Incidentally, this value corresponds closely to most of the experimental results obtained by L. H. Donnell[3] and E. E. Lundquist[7].

The corresponding value of the parameter η which determines the number of waves is equal to 0.225. In case of $R/t = 1\,000$, the number of waves, n, will be 15 which also agrees well with the experimental evidence. For this particular value of the radius to thickness ratio, the number of waves along the circumference decreases from the $n = 26$ at the beginning of the buckling to $n = 15$ at the calculated minimum buckling stress. This gradual increase in the size of waves with the unit shortening is also observed by the experiments reported in an earlier paper[2].

It is particularly interesting, however, to trace the gradual change in the wave pattern during the buckling process. Figs. 6 and 7 show the lines of equal deflection of the wave surfaces corresponding to different equilibrium states for two values of the aspect ratio of the wave pattern, $\mu = 1.0$ and $\mu = 0.5$. These particular equilibrium states are denoted in Figs. 2, 3, 4 and 5 by small circles in order to indicate their relative position during the buckling process. It is seen that there is a rapid shift from the rectangular waves bounded by lines, $x =$ const., and $y =$ const., as predicted by the classical theory for infinitesimal wave amplitudes, to staggered rows of circular or elliptical waves. Whereas, the rectangular waves are directed alternatively inward and outward, the circular or elliptical waves are all directed inward. The transition is practically completed for $\xi = 4$ or 6, i.e., when the wave amplitude is only 4 or 6

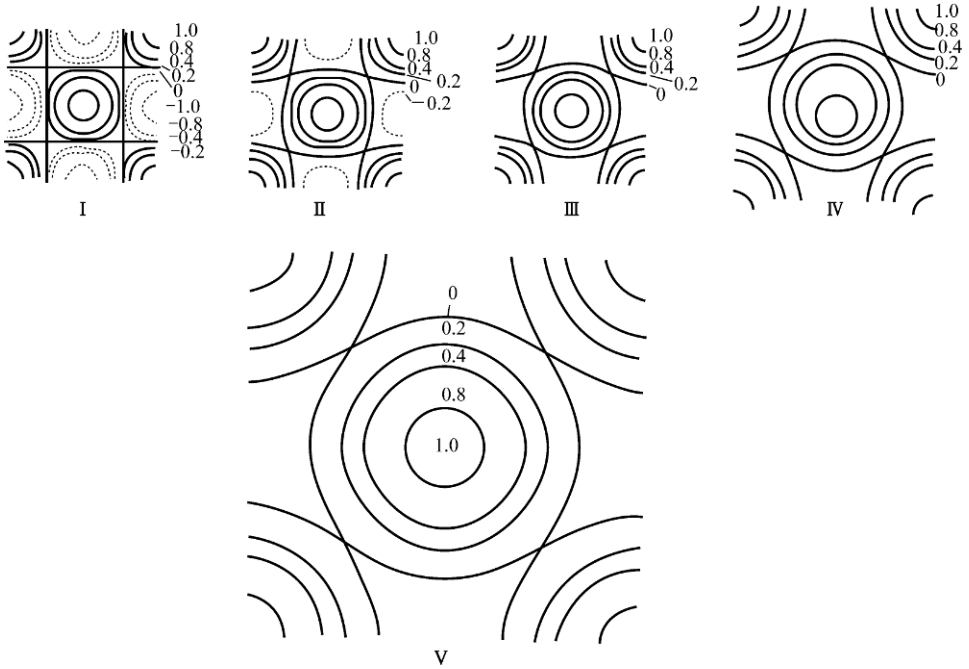


Fig. 6 Lines of equal deflection of wave surfaces. $+1.0$ = maximum inward deflection

Compression in vertical direction

	ξ	$\mu = 1.00$ η
I	0	0.676
II	1.00	0.676
III	2.00	0.676
IV	4.00	0.400
V	16.22	0.100

times the thickness of the shell. The occurrence of such inwardly directed circular and elliptical waves at this stage of the buckling process is in good agreement with the experimental observations[2]. If the experiment is continued to larger deflections ($\xi \sim 60$), these staggered waves acquire the characteristic diamond shape. The present approximate theory fails to give these sharp diamond shaped waves. It is obviously not sufficiently exact for such large deflections. Furthermore, when these diamond shaped waves occur, the load on the specimen actually falls to a very low value such as $\sigma R/(Et) \cong 0.06$, whereas the theory shows a slight increase of the stress at least for the case $\mu = 1.0$. Therefore, the present calculation can be only considered as a fair approximation to the earlier stages of buckling when the wave amplitude is only a few times the thickness of the shell. Nevertheless, it reproduces the characteristic features of the buckling process observed in the laboratory.

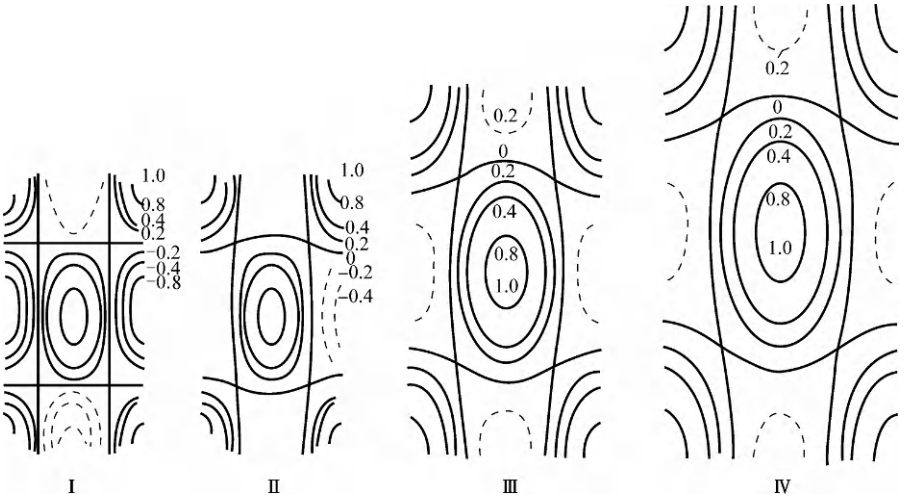


Fig. 7 Lines of equal deflection of wave surfaces. +1.0 = maximum inward deflection

Compression in vertical direction

	ξ	$\mu = 0.500$ η
I	0.00	0.529
II	2.50	0.529
III	5.50	0.289
IV	10.00	0.196

The Effect of the Elastic Characteristic of the testing Machine on the Buckling Phenomenon

It was stated in the previous paragraph that the state of the specimen is determined by the distance between the end plate and that this distance is the independent parameter controlled by the experimenter. This statement is correct only insofar the elasticity in the mechanism of the testing machine is neglected. There is always a certain amount of elastic deflection in the loading mechanism and this deflection is a function of the load. Hence, if, for example, the loading crank is held at a certain position, the compression force acting on the specimen will force the end plates apart and thus reduce the amount of end shortening of the specimen. The actual shortening is determined by the load-deflection characteristics of the specimen and the testing machine. Assuming that the testing machine has a linear elastic characteristic, the compression load is related to the end shortening by parallel straight lines, each line corresponding to, say, a fixed number of turns of the loading crank. If the loading crank of the machine is held at a fixed position, corresponding values of the compression load and end shortening of the specimen must lie on the straight line for this crank position. If the load-end shortening characteristics of the specimen itself are given, it is evident that the equilibrium

positions of the entire system are determined by intersections of the curves representing the characteristics of the specimen with the straight lines representing the characteristics of the machine.

Fig. 8 shows representative curves for the characteristics of the specimen and two families of straight lines representing the characteristics of two different testing machines. It is evident that after the maximum or initial buckling load is reached, the shell will jump to a new equilibrium position involving much lower compression load. But this new equilibrium position is determined not only by the load-end shortening relationship and also by the elastic characteristic of the testing machine. A more elastic machine will give a set of characteristic straight lines with smaller slopes. Therefore, in case of curve A (Fig. 8), a more elastic machine will make the shell to jump to a higher load, while in case of curve B, a more elastic machine will make the shell to jump to a lower load. This influence of the elasticity of the testing machine has been discussed by the senior author in connection with the plastic buckling of columns[8].

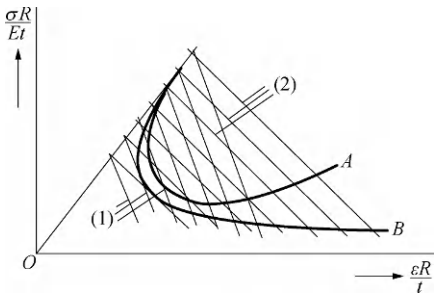


Fig. 8 Effect of rigidity of testing machine on behavior of specimen
(1) Represents a more rigid machine
(2) Represents a less rigid machine

Conclusions

In the previous paragraphs, the authors have shown that there are equilibrium positions with buckled shape involving much lower load than the buckling load predicted by the classical theory, and thus if the specimen is slightly imperfect, it is reasonable to expect much lower buckling loads. They have also pointed out that the elastic characteristic of the testing machine might have quite a large influence on the buckling process and this might be another cause of the large scattering of the data obtained by different experimenters. However, due to the complexity of the problem, the results given in this paper can be only considered as a rough approximation and most of the statements made are qualitative rather than quantitative. To put the new theory on a solid footing, a more accurate solution of the differential equations of equilibrium is necessary. Particular attention must be given to the calculation of the elastic energy stored in the shell, because it is found that the most probable equilibrium depends on

the magnitude of the elastic energy stored in the various equilibrium positions compatible with the constraint exerted by the loading process.

Furthermore, an inquisitive mind will, perhaps, be pleased by a rigorous proof of the validity of all the large deflection equations. These equations are established by intuitive arguments, not by systematic reasoning. For instance, due to the appearance of sharp curvatures in the diamond shaped wave surfaces at large deflections, it is not certain whether the curvature of the shell has to be calculated more accurately by taking into account the second order terms, or the extensions of the median surface should be more accurately determined. It is the belief of the authors that an investigation of these problems by starting from the general non-linear theory of elasticity developed by G. Kirchhoff, J. Boussinesq and others is very desirable. The recent work by R. Kappus[9] is a noteworthy contribution in this field of investigation. The senior author has already expressed this opinion in his 1939 Gibbs Lecture[10] given before the American Mathematical Society.

References

[1] von Kármán Th., Tsien, Hsue-Shen. The Buckling of Spherical Shells by External Pressure. Journal of the Aeronautical Sciences, 1939,7(2): 43.

[2] von Kármán Th., Dunn Louis G., Tsien, Hsue-Shen. The Influence of Curvature on the Buckling Characteristics of Structures. Journal of the Aeronautical Sciences, 1940,7(7): 276.

[3] Donnell L H. A New Theory for the Buckling of Thin Cylinders Under Axial Compression and Bending. A. S. M. E. Transactions, 56:795 – 806,1934.

[4] Flügge W. Die Stabalität der Kreiszylinderschale. Ingenieur Archiv, 1932,(3): 463 – 506.

[5] von Kármán Th. Encyklopädie der Mathematischen Wissenschaften. 1910,Ⅳ.4: 349.

[6] Donnell L H. Stability of Thin-Walled Tubes Under Torsion. N. A. C. A. Technical Report No. 479, 1934.

[7] Lundquist E E. Strength Tests of Thin-Walled Duralumin Cylinders in Compression. N. A. C. A. Technical Report No. 473, 1933.

[8] von Kármán Th. Untersuchungen über Knickfestigkeit. Forschungsarbeiten, Berlin, 1910: 81.

[9] Kappus R. Zur Elastizitätstheorie endlicher Verschiebungen. ZAMM, 1939,19: 271 – 285. 344 – 361.

[10] von Kármán Th. The Engineer Grapples with Nonlinear Problems. Bulletin of the American Mathematical Society, 1940,46: 636 – 637.